Radius, self-induced potential, and number of virtual optical phonons of a polaron

F. M. Peeters
Department of Physics, University of Antwerp (Universitaire Instelling Antwerpen), Universiteitsplein 1, B-2610 Wilrijk-Antwerpen, Belgium

J. T. Devreese
Department of Physics, University of Antwerp (Universitaire Instelling Antwerpen), Universiteitsplein 1, B-2610 Wilrijk-Antwerpen, Belgium; University of Antwerp (Rijksuniversitair Centrum Antwerpen), B-2020 Antwerpen, Belgium; and Department of Physics, Eindhoven University of Technology, NL-5600-MB Eindhoven, The Netherlands
(Received 25 October 1984)

The self-induced polaron potential, the polaron radius, and the number of virtual optical phonons are calculated within the Feynman description of the polaron. The dependence of these quantities on the temperature, the magnetic field strength, and the electron-phonon coupling constant is investigated analytically and numerically.

I. INTRODUCTION

Fröhlich polarons[1] have been the subject of continuous interest during the last forty years. Most of the studies in polarons[2] can be subdivided into two categories: (i) calculation of static quantities such as, e.g., the polaron ground-state energy[3] and the polaron effective mass,[3,4] and (ii) the calculation of dynamical quantities[5] such as, e.g., dc and ac mobility and the nonlinear response to an electric field. Relatively little attention has been devoted in the past to the calculation of the self-induced polaron potential, the polaron radius, and the number of optical phonons present in the virtual-phonon cloud surrounding the electron. To the best of our knowledge such a calculation is only partially available in the literature[6-9] in the case of zero external magnetic field and zero (or very small) lattice temperature. In the present paper we study the self-induced polaron potential, the polaron radius, and the number of virtual optical phonons using an extension[10] of the Feynman polaron theory[3] for arbitrary values of the electron-phonon coupling constant (α), temperature (T), and magnetic field strength ($\mathscr{H}$).

An electron interacting with the vibrational modes of a crystal and a constant uniform magnetic field is described by the Hamiltonian

$$H=\frac{1}{2m}\left[\mathbf{p}+\frac{e}{c}\mathbf{A}\right]^2+\sum_{\mathbf{k}}\hbar\omega_{\mathbf{k}}a_{\mathbf{k}}^{\dagger}a_{\mathbf{k}}+\sum_{\mathbf{k}}(V_{\mathbf{k}}a_{\mathbf{k}}e^{i\mathbf{k}\cdot\mathbf{r}}+V_{\mathbf{k}}^{*}a_{\mathbf{k}}^{\dagger}e^{-i\mathbf{k}\cdot\mathbf{r}}), \quad (1)$$

where we used standard polaron notations (see, e.g., Ref. 2). The magnetic field is chosen along the z axis, and the vector potential will be written in the symmetrical Coulomb gauge: $\mathbf{A}=\frac{1}{2}\mathscr{H}(-y,x,0)$. In the following we will need the partition function $Z=\mathrm{Tr}e^{-\beta\mathscr{H}}$, which, in a path-integral formulation of the trace, becomes

$$Z=\int d\mathbf{r}_0\int_{\mathbf{r}_0=\mathbf{r}(0)}^{\mathbf{r}_0=\mathbf{r}(\beta)}\mathscr{D}\mathbf{r}(u)\,e^{S[\mathbf{r}(u)]}, \quad (2)$$

where (i) we have dropped the contribution of the free phonons to the partition function Z, and (ii) the phonon variables are eliminated exactly. The action $S[\mathbf{r}(t)]$ in Eq. (1) is given by[10] $S=S_e+S_i$, where

$$S_e=\frac{1}{2}\int_0^{\beta}du\left[\frac{[\dot{\mathbf{r}}(u)]^2}{m}+i\omega_c[x(u)\dot{y}(u)-y(u)\dot{x}(u)]\right] \quad (3a)$$

and

$$S_I=\sum_{\mathbf{k}}|V_{\mathbf{k}}|^2\int_0^{\beta}du\int_0^{\beta}ds\,G_{\omega_{\mathbf{k}}}(u-s)e^{i\mathbf{k}\cdot[\mathbf{r}(u)-\mathbf{r}(s)]}, \quad (3b)$$

with $\omega_c=e\mathscr{H}/mc$ the cyclotron frequency and

$$G_{\omega}(u)=\tfrac{1}{2}n(\omega)(e^{\omega|u|}+e^{\omega(\beta-|u|)}) \quad (3c)$$

the phonon Green's function, where $n(\omega)=1/(e^{\beta\hbar\omega}-1)$ is the occupation number of phonons with frequency ω.

The present paper is organized as follows. In Sec. II, we calculate, within our extension[10] of the Feynman polaron model, the following quantities: (i) the self-induced polaron potential, (ii) the number of virtual phonons as a function of wave vector and the total number of virtual phonons, and (iii) the polaron radius along and perpendicular to the magnetic field. The results are intended to be valid for arbitrary electron-phonon coupling, temperature, and magnetic field strength. In Sec. III we present a numerical analysis of the above quantities, and explicit analytic expressions are obtained for limiting values of α, T, and $\mathscr{H}$. In Ref. 10 we found that as a function of the magnetic field strength, the polaron can exhibit a transition from a dressed to a stripped polaron state. At this transition the effective electron-phonon interaction perpendicular to the magnetic field decreases dramatically. The consequence of this transition on the above quantities is also investigated. The conclusion is presented in Sec. IV.

II. GENERAL RESULTS

A. The self-induced polaron potential

The electron interacting with the longitudinal-optical (LO) phonons induces a potential

$$V(\mathbf{x})=\langle\Phi(\mathbf{r}-\mathbf{x})\rangle\ , \tag{4}$$

which is defined as the thermodynamical average over the electrostatic potential operator

$$\Phi(\mathbf{r})=-\frac{1}{e}\sum_{\mathbf{k}}(V_{\mathbf{k}}a_{\mathbf{k}}e^{i\mathbf{k}\cdot\mathbf{r}}+V_{\mathbf{k}}^{*}a_{\mathbf{k}}^{\dagger}e^{-i\mathbf{k}\cdot\mathbf{r}})\ , \tag{5}$$

and which is proportional to the interaction term in the Fröhlich Hamiltonian.[11] Inserting Eq. (5) into Eq. (4) shows that one must calculate the average

$$B_{\mathbf{k}}=\langle a_{\mathbf{k}}e^{i\mathbf{k}\cdot\mathbf{r}}\rangle=\langle a_{\mathbf{k}}^{\dagger}e^{-i\mathbf{k}\cdot\mathbf{r}}\rangle^{*}\ , \tag{6a}$$

which can be expressed in terms of the partition function

$$B_{\mathbf{k}}=-\frac{1}{\beta}\frac{1}{Z}\frac{\partial Z}{\partial V_{\mathbf{k}}}\ . \tag{6b}$$

By inspection of Eqs. (2) and (3a)—(3c), we can write $B_{\mathbf{k}}$ as a path-integral average,

$$B_{\mathbf{k}}=-\frac{1}{\beta}\left\langle\frac{\partial S[\mathbf{r}]}{\partial V_{\mathbf{k}}}\right\rangle\ . \tag{6c}$$

The approximation consists of replacing the weight function $e^{S[\mathbf{r}]}$ in the path-integral average, denoted by $\langle\ \rangle$ in Eq. (6c), by the weight function $e^{S_m[\mathbf{r}]}$, where $S_m[\mathbf{r}]$ is the generalized Feynman polaron-model action introduced in Ref. 10. We then obtain (see Appendix A of Ref. 10)

$$B_{\mathbf{k}}=-V_{\mathbf{k}}^{*}[1+n(\omega_{\mathbf{k}})]\int_0^{\beta}du\,e^{-\omega_{\mathbf{k}}u}e^{-k_z^2D(u)}e^{-k_\perp^2D_H(u)}\ , \tag{6d}$$

with $k_\perp^2=k_x^2+k_y^2$, and

$$D(u)=\frac{w_{\parallel}^2}{v_{\parallel}^2}\frac{u}{2}\left[1-\frac{u}{\beta}\right]+\frac{v_{\parallel}^2-w_{\parallel}^2}{2v_{\parallel}^3}\left[1-e^{-v_{\parallel}u}-4n(v_{\parallel})\sinh^2\left[\frac{v_{\parallel}u}{2}\right]\right]\ , \tag{7a}$$

$$D_H(u)=\sum_{i=1}^{3}d_i^2\left[1-e^{-s_iu}-4n(s_i)\sinh^2\left[\frac{s_iu}{2}\right]\right]\ , \tag{7b}$$

where

$$d_i^2=\frac{1}{2s_i}\frac{s_i^2-w_\perp^2}{3s_i^2+2(-1)^i\omega_cs_i-v_\perp^2},\quad i=1,2,3 \tag{7c}$$

and the eigenfrequencies $s_1\le s_2\le s_3$ are the roots of the cubic equation

$$s(s^2-v_\perp^2)+(-1)^i\omega_c(s^2-w_\perp^2)=0\ .$$

The parameters $(v_{\parallel},w_{\parallel},v_\perp,w_\perp)$ were determined in Ref. 10 by a variational calculation of the polaron free energy.

Inserting the expression (6d) for $B_{\mathbf{k}}$ into the potential (4) results in

$$V(\mathbf{x})=\frac{2}{e}\sum_{\mathbf{k}}|V_{\mathbf{k}}|^2e^{-i\mathbf{k}\cdot\mathbf{x}}[1+n(\omega_{\mathbf{k}})]\times\int_0^{\beta}du\,e^{-\omega_{\mathbf{k}}u}e^{-k_z^2D(u)}e^{-k_\perp^2D_H(u)}\ . \tag{8}$$

Note that $eV(\mathbf{x}=0)=2\langle S_I\rangle/\beta$ equals twice the contribution of the average of the electron-phonon interaction part to the free energy. Limiting ourselves to the case of the optical polaron, i.e., $\omega_{\mathbf{k}}=\omega_0$ and

$$|V_k|^2=\frac{4\pi\alpha}{V}\frac{(\hbar\omega_0)^2}{k^2}\left[\frac{\hbar}{2m\omega_0}\right]^{1/2}\ ,$$

we are able to reduce Eq. (8) to

$$V(r_\perp,z)=\frac{\hbar\omega_0}{e}\alpha\left[\frac{2}{\pi}\right]^{1/2}(1+\bar{n})\int_0^{\beta}du\,e^{-u}\int_0^{1/\sqrt{D(u)}}dt\frac{\exp[-(t^2/4)\{r_\perp^2+z^2/[1+H(u)t^2]\}}{[1+H(u)t^2]^{1/2}}\ , \tag{9}$$

where $r_\perp^2=x^2+y^2$, $H(u)=D(u)-D_H(u)$, and $\bar{n}=n(\omega_0)$ is the occupation number of LO phonons. In Eq. (9), z and $r_\perp$ are in units of $R_D=(\hbar/m\omega_0)^{1/2}$ and temperature is in units of $T_D=\hbar\omega_0/k_B$, with k_B Boltzmann's constant.

B. The average number of virtual phonons

First we calculate the average number of virtual phonons with a wave vector $\mathbf{k}$,

$$N_{\mathbf{k}}=\langle a_{\mathbf{k}}^{\dagger}a_{\mathbf{k}}\rangle\ , \tag{10}$$

where the number of free LO phonons is subtracted [see Eq. (2)]. From the definition of the partition function Z and the explicit form of the Hamiltonian (1), we can write Eq. (10) as

$$N_{\mathbf{k}}=-\frac{1}{\beta\hbar}\frac{1}{Z}\frac{\partial Z}{\partial\omega_{\mathbf{k}}}\ , \tag{11}$$

or in terms of a path-integral average,

$$N_{\mathbf{k}}=-\frac{1}{\beta\hbar}\left\langle\frac{\partial S[\mathbf{r}]}{\partial\omega_{\mathbf{k}}}\right\rangle\ . \tag{12}$$

Inserting the explicit form for the action, Eqs. (3a) and (3b), we find

$$N_{\mathbf{k}}=-\frac{1}{\beta\hbar}|V_{\mathbf{k}}|^2\int_0^\beta du\int_0^\beta ds\frac{\partial G_{\omega_{\mathbf{k}}}(u-s)}{\partial\omega_{\mathbf{k}}}\times\langle\exp\{i\mathbf{k}\cdot[\mathbf{r}(u)-\mathbf{r}(s)]\}\rangle\ . \tag{13}$$

The average in Eq. (13) is the Fourier transform of the electron density-density correlation function for imaginary times. We have calculated this correlation function in Ref. 10 for the case of our generalized Feynman polaron model. The result was

$$\langle\exp\{i\mathbf{k}\cdot[\mathbf{r}(u)-\mathbf{r}(s)]\}\rangle=\exp[-k_\perp^2D_H(u-s)-k_z^2D(u-s)]\ ,$$

which we may insert in Eq. (13),

$$N_{\mathbf{k}}=\frac{|V_{\mathbf{k}}|^2}{\hbar}[1+n(\omega_{\mathbf{k}})]\int_0^\beta du[u+\beta n(\omega_{\mathbf{k}})]\times e^{-\omega_{\mathbf{k}}u}e^{-k_z^2D(u)}e^{-k_\perp^2D_H(u)}\ . \tag{14}$$

In the case of the optical polaron, this expression becomes

$$N_{\mathbf{k}}=\left[\frac{\hbar}{2m\omega_0}\right]^{1/2}\frac{4\pi\alpha}{V}\frac{1}{k^2}(1+\bar{n})\times\int_0^\beta du(u+\beta\bar{n})e^{-u}e^{-k_z^2D(u)}e^{-k_\perp^2D_H(u)}\ , \tag{15}$$

which has the following limit,

$$\lim_{k\to0}N_k=\frac{2\pi\alpha}{k^2}\frac{1}{V}\left[\frac{2\hbar}{m\omega_0}\right]^{1/2}\ ,$$

valid for all α.

The average total number of phonons is

$$N=\sum_{\mathbf{k}}N_{\mathbf{k}}\ , \tag{16}$$

which, in the case of the optical polaron, becomes

$$N=\frac{\alpha}{2\sqrt{2\pi}}(1+\bar{n})\int_0^\beta du\,(u+\beta\bar{n})e^{-u}\frac{1}{\sqrt{H(u)}}\times\ln\left[\frac{\sqrt{D(u)}+\sqrt{H(u)}}{\sqrt{D(u)}-\sqrt{H(u)}}\right]\ . \tag{17}$$

C. The polaron radius

The polaron (in contrast to the electron) is not a pointlike particle, but it has a finite extension in space. The induced polarization charge density $\rho(\mathbf{r})$, which was calculated in Ref. 12, is a measure for the polaron probability distribution

$$p(\mathbf{r})=\rho(\mathbf{r})\Big/\int d\mathbf{r}\rho(\mathbf{r}) \tag{18}$$

around the polaron center. From Eq. (6) of Ref. 12, we obtain, for the optical polaron, within the extended Feynman polaron model (with units for which $\hbar=m=\omega_0=1$),

$$p(\mathbf{r})=\frac{1+\bar{n}}{8\pi^{3/2}}\int_0^\beta du\,\frac{e^{-u}}{\sqrt{D(u)}D_H(u)}e^{-r_\perp^2/4D_H(u)}e^{-z^2/4D(u)}\ . \tag{19}$$

In the case of a spherically symmetric probability distribution [i.e., $\omega_c=0$ and, therefore, $D(u)=D_H(u)$], we can define a radius R_H,

$$1/R_H=\langle 1/|\mathbf{r}|\rangle\ , \tag{20}$$

where the average is over the function $p(\mathbf{r})$. One easily finds

$$\frac{1}{R_H}=\frac{1}{\sqrt{\pi}}\int_0^{\beta/2}du\frac{1}{\sqrt{D(u)}}\frac{\cosh(\beta/2-u)}{\sinh(\beta/2)}\ , \tag{21}$$

where R_H is expressed in units of $R_D=\sqrt{\hbar/m\omega_0}$. When a magnetic field is applied, the spherical symmetry is broken and the problem has cylindrical symmetry. Then we can define a radius, respectively, along ($R_{||}$) and perpendicular ($R_\perp$) to the magnetic field. In such a situation it is no longer meaningful to define a radius R_H in the sense of Eq. (20). For example, if one defines $1/R_{||}=\langle 1/|z|\rangle$, one finds $1/R_{||}=\infty$.

Therefore we have adopted another definition for the polaron radius which measures the mean-square deviation of the electron from the polaron center; explicitly,

$$R_{||}=(\langle z^2\rangle)^{1/2} \tag{22a}$$

and

$$R_\perp=(\langle r_\perp^2\rangle/2)^{1/2}\ . \tag{22b}$$

Using the probability function (19), one obtains

$$R_{||}^2=2(1+\bar{n})\int_0^\beta du\,e^{-u}D(u) \tag{23a}$$

and

$$R_\perp^2=2(1+\bar{n})\int_0^\beta du\,e^{-u}D_H(u)\ , \tag{23b}$$

which can be written in closed form,

$$R_{||}^2=\frac{w_{||}^2}{v_{||}^2}\left[1-\frac{2}{\beta}+2\bar{n}\right]+\frac{v_{||}^2-w_{||}^2}{v_{||}^2(1+v_{||})}\left[1+\frac{2}{v_{||}-1}[v_{||}n(v_{||}-\bar{n})]\right] \tag{24a}$$

and

$$R_\perp^2=2\sum_{i=1}^3 d_i^2\frac{s_i}{1+s_i}\left[1+\frac{2}{s_i-1}[s_in(s_i)-\bar{n}]\right]\ , \tag{24b}$$

where $R_{||}$ and $R_\perp$ are in units of R_D.

III. NUMERICAL RESULTS AND ANALYTIC RESULTS FOR LIMITING VALUES OF α, T, AND $\mathscr{H}$

To analyze the behavior of the potential $V(\mathbf{x})$, the number of phonons $N_{\mathbf{k}}$, N, and the polaron radius $R_{||}$,$R_\perp$ as a function of the electron-phonon coupling constant α, temperature T, and magnetic field $\mathscr{H}$, we proceed in the

following way. First, the case $T=\mathscr{H}=0$ is considered and the α dependence is studied. Next, the T dependence is studied for $\mathscr{H}=0$ and fixed α. Finally, we consider the case $T=0$, α fixed, and study the magnetic field dependence. Special attention is paid in the last case to the recently predicted[10] stripping transition of the polaron. We will use units such that $\hbar=m=\omega_0=1$.

A. Dependence on the electron-phonon coupling strength

If one chooses $\mathscr{H}=0$, it follows that $v_\perp=v_\parallel=v$, $w_\perp=w_\parallel=w$, which implies that $D(u)=D_H(u)$. In this limit, $V(r)$ and N can be simplified considerably,

$$V(r)=\frac{\hbar\omega_0}{e}\frac{\sqrt{2\alpha}}{r}(1+\bar{n})\int_0^\beta du\, e^{-u}\mathrm{erf}\left[\frac{r}{2\sqrt{D(u)}}\right], \quad (25)$$

$$N=\frac{\alpha}{\sqrt{2\pi}}(1+\bar{n})\int_0^\beta du\frac{e^{-u}}{\sqrt{D(u)}}(u+\beta\bar{n}), \quad (26)$$

where $\mathrm{erf}(x)$ is the error function.

In Fig. 1 the self-induced potential $\tilde{V}(R)=V(r)e/2\alpha m\omega_0^2$ at $T=\mathscr{H}=0$ is plotted as a function of the distance from the polaron center for different values of the electron-phonon coupling constant. The number of virtual phonons, scaled by

$$N_0=\frac{1}{V}\left[\frac{\hbar}{m\omega_0}\right]^{1/2}\frac{1}{k^2},$$

is shown in Fig. 2(a) as a function of the wave vector. The wave vector is in units of $k_B=(m\omega_0/\hbar)^{1/2}$. The average total number of virtual phonons as a function of α is plotted in Fig. 2(b). The polaron radius (in units of R_D) for two different definitions of the radius [see Eqs. (20) and (22a)] and for the Feynman polaron model itself (dashed curve) is plotted in Fig. 3 as a function of the electron-phonon coupling for $T=\mathscr{H}=0$. The radius of the Feynman polaron model was obtained by Schultz,[7]

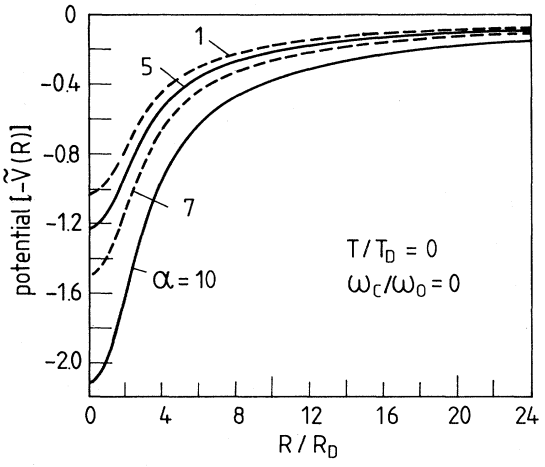

FIG. 1. Self-induced polaron potential $V(R)$ as a function of the distance from the polaron center at zero temperature and zero magnetic field, and for different values of the electron-phonon coupling constant. $\tilde{V}(R)=V(R)e/2\alpha m\omega_0^2$ and $R_D=(\hbar/m\omega_0)^{1/2}$.

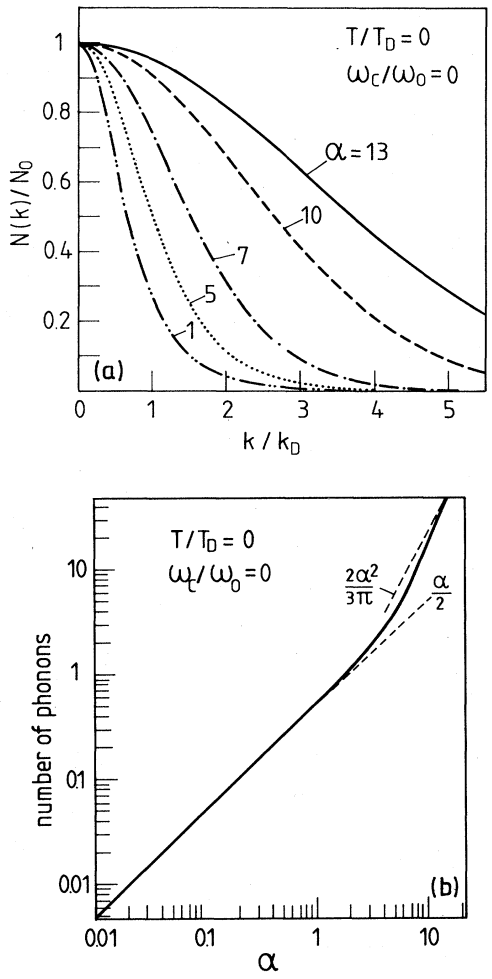

FIG. 2. (a) Number of virtual phonons as a function of the wave vector for the same situation as in Fig. 1. (b) Average total number of virtual LO phonons as a function of the electron-phonon coupling α for $T=0$ and $\omega_c=0$. $N_0=(\hbar/m\omega_0)^{1/2}/k^2V$ and $k_D=(m\omega_0/\hbar)^{1/2}$.

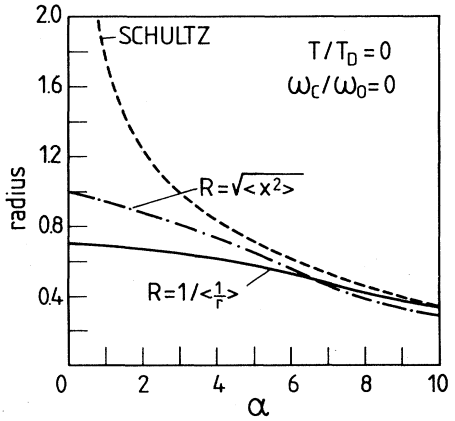

FIG. 3. Polaron radius, in units of $R_D=(\hbar/m\omega_0)^{1/2}$, as a function of the electron-phonon coupling at $T=0$ and $\omega_c=0$, and for three different definitions of the polaron radius.

$$R_F=\left[\frac{3}{2}\frac{v}{v^2-w^2}\right]^{1/2}, \tag{27}$$

with v and w the variational parameters of the Feynman model.

The behavior of the different curves in Figs. 1–3 will be discussed in terms of the analytic expressions for the limiting behavior for $\alpha \ll 1$ and $\alpha \gg 1$.

(a) $\alpha \ll 1$. Then $v \approx w$ and, consequently,

$$D(u)=D_H(u)=(u/2)(1-u/\beta) .$$

For $T=0$ we find, for the potential,

$$V(r)=\frac{\sqrt{2}\alpha}{r}(1-e^{-\sqrt{2}r}) , \tag{28}$$

which is finite at the polaron center, i.e., $V(0)=2\alpha$, and which is exactly *twice* the polaron ground-state energy. At large distances from the polaron center, Eq. (28) reduces to a Coulomb potential $V(r)\simeq\sqrt{2}\alpha/r$ which can be written as

$$V(r)\simeq e\left[\frac{1}{\epsilon_\infty}-\frac{1}{\epsilon_0}\right]\frac{1}{r}$$

[ϵ_0 (ϵ_∞) is the static (high-frequency) dielectric constant]. This is the result to be expected from classical electrostatics.

The average number of virtual LO phonons with wave vector k equals

$$N(k)=\frac{2\sqrt{2}\pi\alpha}{k^2(1+k^2/2)^2} , \tag{29}$$

from which one obtains, for the average total number of phonons,

$$N=\alpha/2 , \tag{30}$$

which is a result already obtained by Lee *et al.* in Ref. 6.

For the polaron radius, we find

$$R_H=\left\langle\frac{1}{r}\right\rangle^{-1}=\frac{1}{\sqrt{2}}(1-\tfrac{2}{81}\alpha+\cdots) , \tag{31a}$$

$$R=(\langle r^2\rangle/3)^{1/2}=1-\alpha/18+\cdots , \tag{31b}$$

and[7]

$$R_F=\tfrac{3}{2}(3/2\alpha)^{1/2} \tag{31c}$$

R_H and R are limited by the quantum fluctuations of the LO-phonon field. R_F diverges for $\alpha\to 0$, because in this limit it measures the extent of a quasifree particle.

(b) $\alpha \gg 1$. In this limit, $w\to 1$, $v\to 4\alpha^2/9\pi$, and $D(u)\simeq(1-e^{-vu})/2v$. The potential becomes

$$V(r)=2\alpha(v/\pi)^{1/2}e^{-r^2v/2}\,{}_1F_1(1;\tfrac{3}{2};\tfrac{1}{2}vr^2) , \tag{32}$$

with ${}_1F_1(a;b;z)$ the degenerate hypergeometric function. At the center of the polaron we find $V(0)=4\alpha^2/3\pi$, which is *4 times* the polaron ground-state energy. For large distances from the polaron center, i.e., $r\gg(\pi/2)^{1/2}(3/\alpha)$, the same result is found as in the case of weak electron-phonon coupling, namely $V(r)=\sqrt{2}\alpha/r$. The average number of phonons with wave vector k is

$$N(k)=\frac{2\sqrt{2}\pi\alpha}{k^2}e^{-(9\pi/8\alpha^2)k^2}\left[1-\frac{9\pi}{4\alpha^2}k^2+\cdots\right] , \tag{33}$$

which gives, for the total number of phonons,

$$N=2\alpha^2/3\pi . \tag{34}$$

The polaron radius is given by

$$R_H=\frac{3\pi}{2\sqrt{2}}\frac{1}{\alpha} \tag{35a}$$

and[7]

$$R=R_F=\tfrac{3}{2}(\sqrt{\pi}/\alpha) , \tag{35b}$$

which have all the same α dependence, but have different coefficients. From Eq. (32) we observe that, for $\alpha\gg 1$, a new scale is introduced in coordinate space, namely $r\sim\sqrt{2/v}=\sqrt{\pi/2}(3/\alpha)$, which is also apparent from Eqs. (35a) and (35b). In wave-vector space the scale [see Eq. (33)] is given by $k=\frac{2}{3}\sqrt{2/\pi}\alpha$.

B. Dependence on temperature

In Fig. 4 the self-induced potential is plotted for different values of the temperature for $\alpha=3$ and $\mathscr{K}=0$. The potential becomes deeper as the temperature increases. Presumably, this is a consequence of the fact that with increasing temperature the lattice becomes more easily polarizable. This result is consistent with the results of Ref. 12 for the temperature dependence of the polarization charge density around the electron.

The number of virtual phonons as a function of the phonon wave vector is shown in Fig. 5(a) for $\alpha=3$ and $\mathscr{K}=0$, and for different values of the lattice temperature. The average total number of phonons for $\mathscr{K}=0$ and $\alpha=1$ and 3 is plotted in Fig. 5(b) as a function of temperature. The increase of the number of short-wavelength phonons with increasing temperature is apparent from Fig. 5(a).

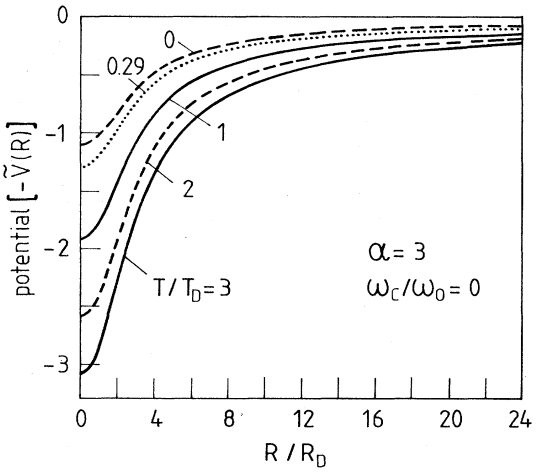

FIG. 4. Same as Fig. 1, but now for a fixed electron-phonon coupling constant, i.e., $\alpha=3$, but for different values of the lattice temperature. $T_D=\hbar\omega_{\rm LO}/k_B$.

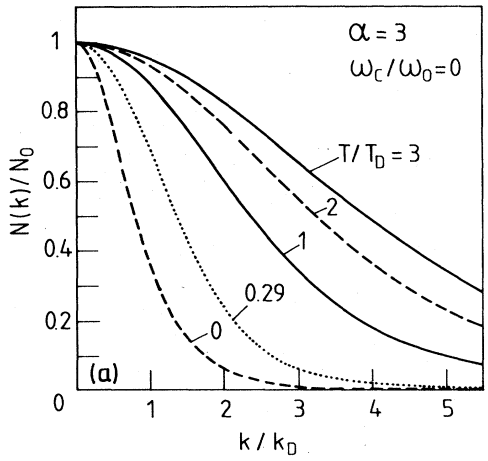

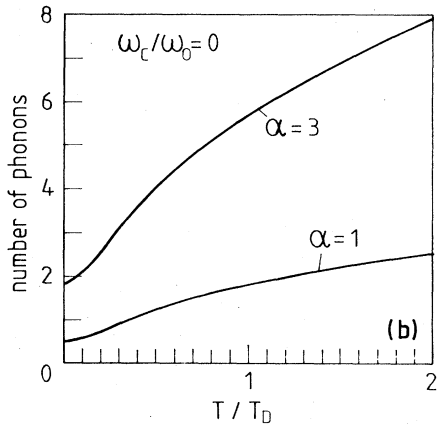

FIG. 5. Same as Fig. 2, but now for a fixed α value and for variable lattice temperature.

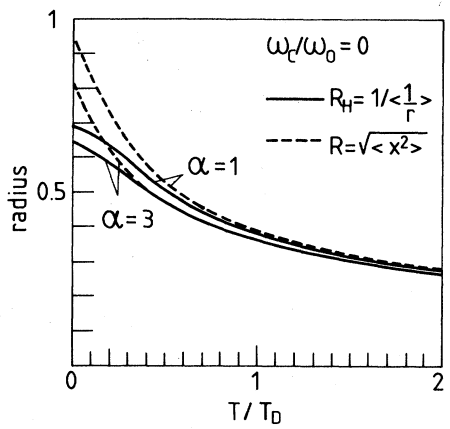

FIG. 6. Polaron radius, in units of $R_D=(\hbar/m\omega_0)^{1/2}$, as a function of the lattice temperature at zero magnetic field, for two values of the electron-phonon coupling, i.e., $\alpha=1$ and 3, and for two different definitions of the polaron radius.

The total number of virtual phonons increases with temperature, and the increase is more pronounced if the electron-phonon coupling is larger, as is seen in Fig. 5(b).

The polaron radius decreases with increasing temperatures, as is shown in Fig. 6. This trend, although surprising at first, is consistent with the temperature behavior of the self-induced polaron potential (Fig. 4) and the induced polarization charge density (see Ref. 12).

Analytically, we will consider only the limit for small electron-phonon coupling strength and for small ($\beta\gg1$) and high temperature ($\beta\ll1$).

(a) $\beta\gg1$. From Eq. (25) we obtain, for the low-temperature correction to the zero-temperature potential of Eq. (28),

$$+\frac{\alpha}{2\beta}(1+\sqrt{2}r)e^{-\sqrt{2}r},$$

which leads to the following expression for the potential around the polaron center:

$$V(r)=2\alpha\left[\left[1+\frac{1}{4\beta}+\cdots\right]-\frac{r}{\sqrt{2}}(1+\cdots)+\frac{r^2}{3}\left[1-\frac{3}{4\beta}+\cdots\right]+\cdots\right]. \tag{36}$$

Note that the $r=0$ temperature correction to $V(r)$ is identical to the temperature correction to the polaron free energy [see Eq. (79) of Ref. 10].

For the number of virtual phonons with wave vector k, the following low-temperature expression is obtained:

$$N(k)=\frac{2\sqrt{2}\pi\alpha}{k^2(1+k^2/2)^2}\left[1+\frac{1}{\beta}\frac{k^2}{(1+k^2/2)^2}+\frac{15}{\beta^2}\frac{k^4}{(1+k^2/2)^4}+\cdots\right]. \tag{37}$$

From Eq. (26) we obtain, for the temperature dependence of the number of phonons in the weak-coupling limit,

$$N=\alpha\sqrt{\pi}\beta^{3/2}(1+\bar{n})e^{-\beta/2}[\tfrac{1}{2}I_0(\beta/2)-\tfrac{1}{2}I_1(\beta/2)+\bar{n}I_0(\beta/2)], \tag{38}$$

which is valid for arbitrary temperature [the $I_n(x)$ are Bessel functions of an imaginary argument]. In the low-temperature limit, Eq. (38) reduces to

$$N=\frac{\alpha}{2}\left[1+\frac{3}{4}\frac{1}{\beta}+\cdots\right]. \tag{39}$$

For the polaron radius we obtain the following results:

$$R_H=\frac{1}{\sqrt{2}}\left[\left[1-\frac{1}{4\beta}+\cdots\right]-\frac{2\alpha}{81}\left[1+\frac{5}{6}\frac{1}{\beta}+\cdots\right]+\cdots\right] \tag{40a}$$

and

$$R=\left[1-\frac{1}{\beta}+\cdots\right]-\frac{\alpha}{18}\left[1-\frac{1}{3\beta}+\cdots\right]+\cdots . \tag{40b}$$

(b) $\beta \ll 1$. At the polaron center the potential is finite,

$$V(0)=2\alpha\left[\frac{\pi}{\beta}\right]^{1/2}\left[1+\frac{\beta^2}{48}+\cdots\right] . \tag{41a}$$

At large distances from the polaron center, such that $r \gg \sqrt{2\beta}$, the potential reduces to a Coulomb potential,

$$V(r)\simeq\sqrt{2}\alpha(1+\bar{n})(1/r) . \tag{41b}$$

For the number of phonons, we find

$$N(k)=\frac{2\sqrt{2}\pi\alpha}{k^2}\left[1-\beta\frac{k^2}{12}+\beta^2\frac{k^4}{240}+\cdots\right] , \tag{42a}$$

which is valid for $k \ll \sqrt{2/\beta}$. The average total number of phonons becomes

$$N=\frac{\alpha\sqrt{\pi}}{\sqrt{\beta}}\left[1-\frac{\beta^2}{48}+\cdots\right] . \tag{42b}$$

In the high-temperature limit the polaron radius,

$$R_H=\sqrt{\beta/2\pi}+\cdots , \tag{43a}$$

$$R=\sqrt{\beta/6}+\cdots , \tag{43b}$$

is essentially determined by the temperature fluctuations and not by the electron-phonon coupling constant.

C. Magnetic field dependence

A magnetic field breaks the spherical symmetry and the resulting problem has axial symmetry. The self-induced polaron potential is plotted in Fig. 7 for $\alpha=3$, $T=0$, and a magnetic field strength corresponding to $\omega_c/\omega_0=3$. The potential is plotted in the direction parallel, i.e., $V(R_\perp=0,z)$, and perpendicular, i.e., $V(R_\perp,z=0)$, to the magnetic field. For comparison, also the result for $\omega_c/\omega_0=0$ is plotted. We remark that at $(R_\perp=0,\ z=0)$ and at large distances from the polaron center, there is no asymmetry. The number of virtual LO phonons is plotted in Fig. 8(a) as a function of the wave vector for $\alpha=3$, $T=0$, and $\omega_c/\omega_0=3$, both for parallel, i.e., $N(k_\perp=0,k_z)$, and perpendicular, directions, i.e., $N(k_\perp,k_z=0)$. Perpendicular to the direction of the magnetic field, the number of short- and intermediate-wavelength phonons is enhanced because of the increasing localization of the electron in this direction. The average total number of virtual phonons increases with magnetic field, as is illustrated in Fig. 8(b). The polaron radius decreases with increasing magnetic field, as shown in Fig. 9. The decrease is faster in the direction perpendicular to the magnetic field. In the perpendicular direction, the magnetic field localizes the electron, and in the limit of large magnetic fields there is almost no dependence on α. The decrease of $R_{||}$ is a consequence of the electron-phonon interaction which tends to restore the spherical symmetry of the pho-

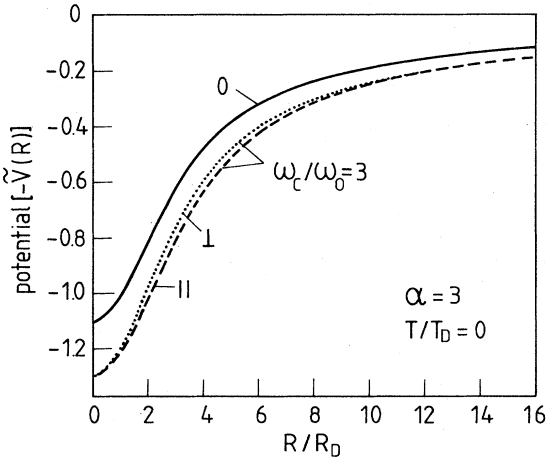

FIG. 7. Self-induced polaron potential as a function of the distance from the polaron center at $\alpha=3$ and $T=0$, and for two values of the magnetic field, i.e., $\omega_c/\omega_0=0$ and 3. For $\omega_c/\omega_0=3$ the potential is plotted in the direction parallel (||) and perpendicular (⊥) to the magnetic field.

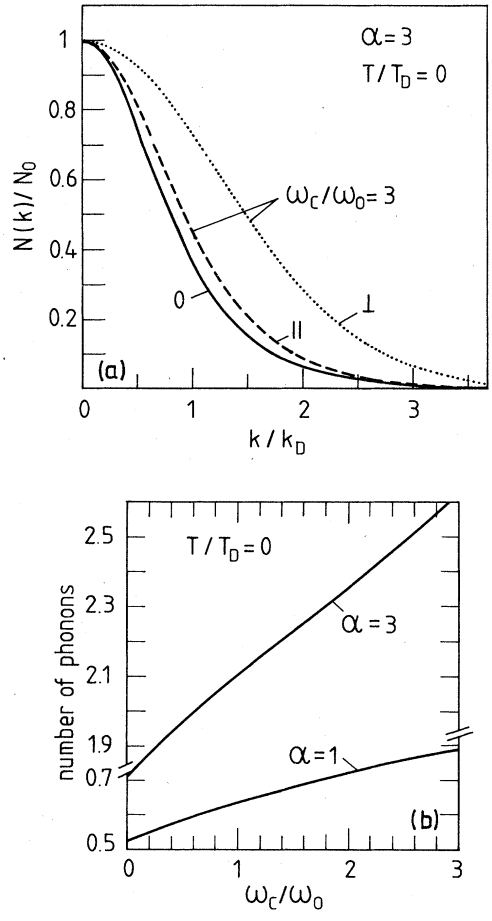

FIG. 8. Same as Fig. 2, but now we fixed α and varied the magnetic field. For $\omega_c/\omega_0=3$, $N(k)$ [panel (a)] is plotted for wave vectors parallel (||) and perpendicular (⊥) to the direction of the magnetic field.

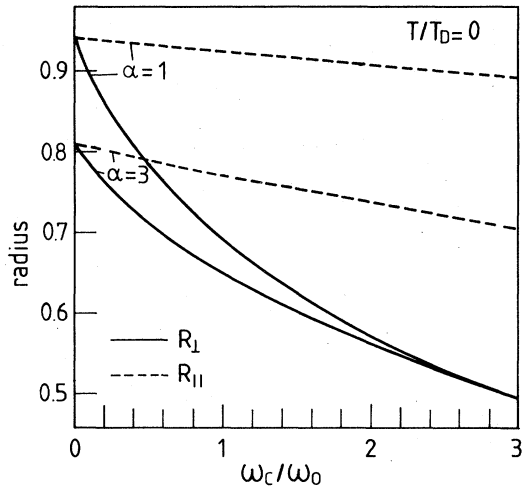

FIG. 9. Polaron radius in the direction parallel ($R_{||}$) and perpendicular ($R_{\perp}$) to the magnetic field as a function of the magnetic field strength for $T=0$ at $\alpha=1$ and 3.

non cloud and, as a consequence, $R_{||}$ depends strongly on α.

In the weak-coupling limit and for $T=0$, we have $D(u)=u/2$ and $D_H(u)=(1-e^{-\omega_c u})/2\omega_c$. The analytic expression for the potential for limiting values of ω_c will not be given here because of its complexity, which is a consequence of the double integral in Eq. (9). The number of LO phonons with wave vector k for $\omega_c/\omega_0 \ll 1$ is given by

$$N(k)=\frac{2\sqrt{2}\pi\alpha}{k^2(1+k^2/2)^2}\left[1+\frac{3}{2}\omega_c\frac{k_{\perp}^2}{(1+k^2/2)^2}+\cdots\right] \tag{44a}$$

and

$$N(k)=\frac{2\sqrt{2}\pi\alpha}{k^2}e^{-k_{\perp}^2/2\omega_c}\left[\frac{1}{(1+k_z^2/2)^2}+\frac{k_{\perp}^2}{2\omega_c}\times\frac{1}{(1+\omega_c+k_z^2/2)^2}+\cdots\right], \tag{44b}$$

for $\omega_c \gg 1$, where $k_{\perp}^2=k_x^2+k_y^2$. The axial symmetry of the problem is apparent from Eqs. (44a) and (44b). We also note the enhanced number of virtual LO phonons with wave vector directed perpendicular to the magnetic field when the magnetic field increases. The average total number of phonons is given by

$$N=\frac{\alpha}{2}\left[1+\frac{\omega_c}{3}+\cdots\right], \quad \omega_c/\omega_0 \ll 1 \tag{45a}$$

and

$$N=\frac{\alpha}{4}[\ln\omega_c+(2-C)+\cdots], \quad \omega_c/\omega_0 \gg 1 \tag{45b}$$

where $C=0.5772\ldots$ is the Euler constant. The polaron radii for $\omega_c/\omega_0 \ll 1$ is given by

$$R_{||}=(1+\cdots)-\frac{\alpha}{18}(1+\tfrac{3}{10}\omega_c+\cdots), \tag{46a}$$

$$R_{\perp}=\left[1-\frac{\omega_c}{2}+\cdots\right]-\frac{\alpha}{18}(1+\tfrac{41}{15}\omega_c+\cdots), \tag{46b}$$

and, for $\omega_c/\omega_0 \gg 1$, it becomes

$$R_{\perp}=1/\sqrt{1+\omega_c}\ . \tag{46c}$$

Recently,[10] we found, within the Feynman approximation and using an anisotropic Feynman polaron model, that for a well-defined critical magnetic field the polaron exhibits a discontinuous transition from a dressed polaron state to a two-dimensional "stripped" state when $\alpha > 4.2$ at $T=0$. The transition is accompanied by a dramatic decrease of the effective electron-phonon interaction in the plane perpendicular to the magnetic field. The influence of this transition on the different quantities characterizing the polaron and under study here, is shown in Figs. 10–12. In these figures we considered, as an example, the situation for $\alpha=7$, $T=0$, and $\omega_c/\omega_0=4.33$. For these parameters the potential is depicted in Fig. 10 for the "stripped" state [solid curve gives $V(R_{\perp},z=0)$ and the dashed curve gives $V(R_{\perp}=0,z)$] and the dressed polaron state [dashed-dotted curve, $V(R_{\perp},z=0)$; dotted curve, $V(R_{\perp}=0,z)$]. Note that in the "stripped" state the potential is not as deep as it is in the dressed state, and that in both states the potential is asymmetrical. The number of virtual LO phonons is plotted as function of the wave vec-

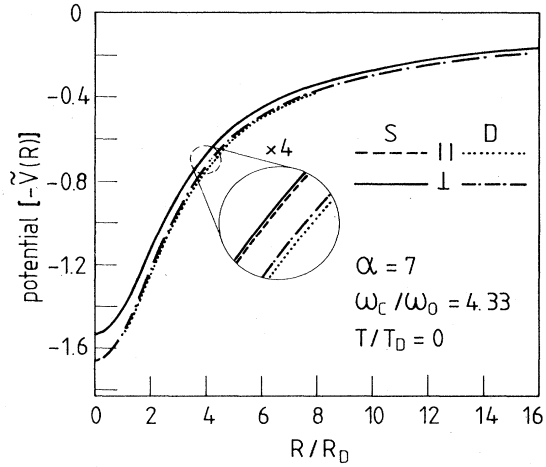

FIG. 10. Self-induced polaron potential in the direction parallel (||) and perpendicular ($\perp$) to the magnetic field for $\alpha=7$, $T=0$, and $\omega_c/\omega_0=4.33$ when the polaron is in the dressed state (D) and in the stripped state (S).

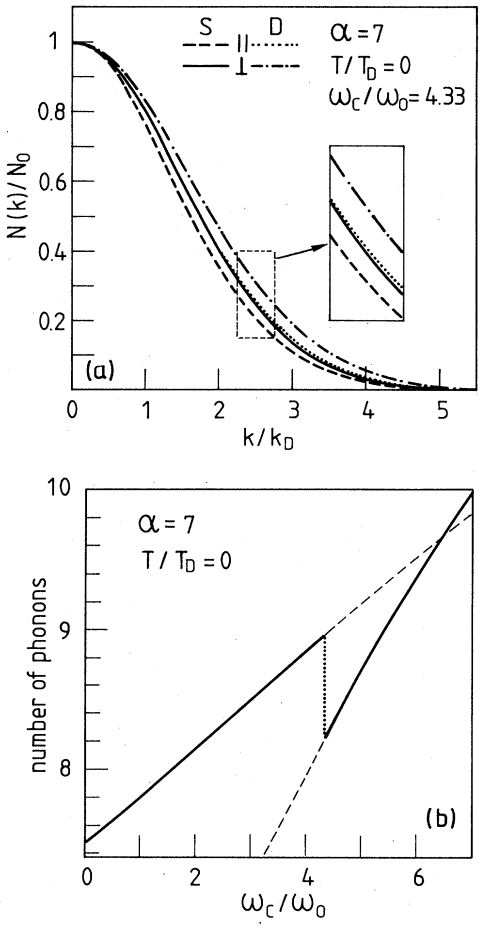

FIG. 11. (a) Number of virtual LO phonons as a function of the wave vector for the same situation as in Fig. 10. (b) Average total number of virtual LO phonons as a function of the magnetic field for $\alpha=7$ and $T=0$. Solid lines correspond to the stable state.

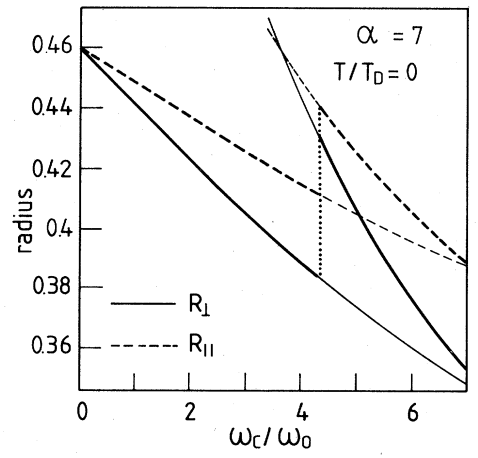

FIG. 12. Polaron radius in the direction parallel ($R_{\|}$) and perpendicular ($R_{\perp}$) to the magnetic field vs ω_c for $\alpha=7$ and $T=0$. The bold solid curves correspond to the stable state.

tor in Fig. 11(a). In this figure we used the same notations for the different curves as in Fig. 10. The average total number of LO phonons is shown in Fig. 11(b). From Figs. 11(a) and 11(b) we note that at the transition point from the dressed polaron state to the "stripped" polaron state, the number of virtual phonons decreases suddenly and the polaron radius (see Fig. 12) increases. The "stripped" state is therefore less confined than the dressed polaron state, which is, e.g., reflected in a small number of virtual LO phonons present.

IV. CONCLUSION

In the present paper we studied the self-induced polaron potential, the average number of virtual LO phonons, and the polaron radius within a generalization of the Feynman polaron model. The dependence of these quantities on the electron-phonon coupling constant, temperature, and magnetic field strength was studied analytically and numerically.

The temperature dependence of the present results is contrary to intuitive expectations (see, e.g., Ref. 9). Intuitively, one might expect that the contribution of the electron-phonon interaction to the different quantities decreases with increasing temperature due to a loss of coherence between the electron and the phonons because of the increase of random temperature fluctuations. The results plotted in Figs. 4, 5(a), 5(b), and 6 indicate that this is not so: the contribution of the electron-phonon interaction increases with increasing temperature.

What one overlooks in the intuitive argument is the fact that the contribution of the electron-phonon interaction to $V(r)$, N_k, N, and R is a measure of the coherence between the motion of the electron and the phonons *only* when the temperature is zero. For nonzero temperature, another aspect of the problem comes into play: (1) the crystal can be polarized much easier, and (2) the electron can also interact with real phonons. The number of real LO phonons increases with increasing temperature and, as a consequence, the electron can interact with more phonons, which probably leads to the observed increase of the contribution of the electron-phonon interaction to $V(r)$, N_k, and N with increasing temperature.

The decrease of the polaron radius with increasing temperature (see Fig. 6) is due to the temperature fluctuations of the phonon field and is not a direct consequence of the electron-phonon interaction. These fluctuations hinder the electron motion, which leads to a reduction of the polaron radius.

ACKNOWLEDGMENTS

One of us (F.M.P.) acknowledges support from the Nationaal Fund for Scientific Research (Nationaal Fonds voor Wetenschappelijk Onderzoek), Belgium. This work was partially sponsored by the Fonds voor Kollektief Fundamenteel Onderzoek (FKFO), Belgium, under Project No. 2.0072.80.

[1]H. Frölich, Adv. Phys. **3**, 325 (1954).
[2]For a recent review, see *Polarons and Excitons in Polar Semiconductors and Ionic Crystals,* edited by J. T. Devreese and F. M. Peeters (Plenum, New York, 1984).
[3]R. P. Feynman, Phys. Rev. **97**, 660 (1955).
[4]D. M. Larsen, Phys. Rev. **174**, 1046 (1968); J. Röseler, Phys. Status Solidi B **25**, 311 (1968); A. Kholodenko and K. F. Freed, Phys. Rev. B **27**, 4586 (1983); **29**, 3711 (1984); K. Arisawa and M. Saitoh, Phys. Status Solidi B **120**, 361 (1983); D. M. Larsen, Phys. Rev. B **29**, 3710 (1984).
[5]For a recent review see F. M. Peeters and J. T. Devreese, in *Solid State Physics,* edited by H. Ehrenreich, D. Turnbull, and F. Seitz (Academic, New York, 1984), Vol. 38, p. 81.
[6]T. D. Lee, F. E. Low, and D. Pines, Phys. Rev. **90**, 297 (1953).
[7]T. D. Schultz, Phys. Rev. **116**, 526 (1959).
[8]H. Shoji and N. Tokuda, J. Phys. C **14**, 1231 (1981).
[9]V. K. Fedyanin and C. Rodriguez, Phys. Status Solidi B **110**, 105 (1982).
[10]F. M. Peeters and J. T. Devreese, Phys. Rev. B **25**, 7281 (1982); **25**, 7302 (1982).
[11]T. D. Lee, F. E. Low, and D. Pines, Phys. Rev. **90**, 297 (1953).
[12]F. M. Peeters and J. T. Devrees, Phys. Status Solidi B **115**, 285 (1983).